Processing salt-encapsulated tantalum nanoparticles for high purity, ultra high surface area applications

J. L. Barr[1,2,*], R. L. Axelbaum[1] and M. E. Macias[1,3]
[1]*Washington University, St. Louis, MO, 63130, USA;* [2]*Pacific Northwest National Laboratory, Richland, WA, 99352, USA;* [3]*MSC Software Corporation, Ann Arbor, MI 48105, USA;* *Author for correspondence (E-mail: jonathan.barr@pnl.gov)*

Abstract

In this study a process for removing the protective encapsulate from salt encapsulated nanopowders has been developed and tested for tantalum nanopowder produced by sodium/halide gas-phase combustion synthesis. A sodium/halide flame can be used to produce salt-encapsulated nanoparticles for many metal and nonoxide ceramic materials. The salt encapsulate allows for control of size and morphology, and protects the core particles from oxygen contamination. Without a protective coating, non-oxide nanopowders can be pyrophoric or form a surface oxide. Despite the beneficial attributes of the NaCl encapsulate, it can also be a source of contamination. Thus, a method by which the encapsulate can be removed and the exposed particles subsequently processed without exposure to environmental contamination was developed. A two step process was developed, where the bulk of the salt is sublimed from the core particles at 880°C and directed out of the system with an inert gas flow followed by a vacuum sublimation at temperatures at or greater than 1200°C for 120 min. These conditions reduced Na and Cl concentrations to below detectable limits of their respective analyses (5 ppm Na and 20 ppm Cl). Heat treating the core particles for 120 min at 1200°C, 1400°C and 1600°C coarsened the particles from 30 nm to approximately 250 nm, 400 nm and 3μm, respectively. At 1600°C a fully dense Ta consolidate was produced by applying a uniaxial load of 45 MPa pressure for 210 min.

Introduction

When the grain sizes of materials are reduced to the nanometer size regime, significant material property enhancements can be observed. Due to the high surface to volume ratio of nanostructured materials, they show great promise for improving material properties that are functions of, for example, chemical reactivity, magnetic moment, polarizability, and geometric structure (Jena et al., 1996). Nanostructured materials show promise in improving thermal barrier materials, battery or capacitor elements, pharmaceutical separations, and energy storage/separation technologies (e.g., gas storage for fuel cell applications) (Cox, 1999).

There are two approaches to producing nanostructured materials: "top down" and "bottom up". With the top down approach, small structures are created from larger ones and then are formed into the final material. Ball milling and grinding in stirred-media mills are examples of this approach (Cho et al., 1996). With the bottom up approach the nanostructured building blocks, such as nanopowders, are formed directly and then a final material is created. Methods such as wet chemical synthesis, gas condensation, and gas phase combustion synthesis are examples of the

12

bottom up approach. Unfortunately, the enormous specific surface area is a major obstacle to the development of non-oxide nanostructured materials. Metals or non-oxide ceramics that are stable as coarse-grained powder or in bulk form, can be highly reactive in the form of nanopowders due to small diffusion distances and because a large volume of the powder is composed of highly reactive surface material (Andrievski, 1994; Groza & Dowding, 1996). Nanoparticles are also more likely to adsorb molecules or ions to stabilize the particles by reducing surface free energy (Zhang et al., 1999). Thus, it is necessary to limit powder exposure to oxygen, moisture, or other reactive materials. For the so-called valve materials, such as Ta and Al, a small oxide layer forms and acts to passivate the surface and prevent subsequent surface reactivity. For micron-sized particles this surface layer contributes minimally to the total amount of impurities. On the other hand, an oxide layer on the surface of a nanostructured particle can account for a considerable percentage of the bulk. Significant oxygen contamination can occur as a result of exposing unprotected powders for even a short time in an inert-gas atmosphere (Shriver & Drezdzon, 1986). Thus, particle contamination due to exposure to oxygen or moisture presents a problem even with methods where the particles are protected in a post-synthesis step (Shriver & Drezdzon, 1986; Groat & Mrox, 1994; Axelbaum et al., 1995). Another challenge to processing nanostructured materials is retaining the nanostructured features because they can be altered by agglomeration and rapid grain growth at high temperature (Groza & Dowding, 1996; Weissmuller, 1996). Self- and impurity-diffusion can be orders of magnitude higher in nanostructured materials than in traditional materials (Haber & Buhro, 1998).

The sodium/halide gas-phase (flame) combustion synthesis and encapsulation process (SFE) is a novel method for producing nanostructured materials that can overcome many of the challenges confronting application of non-oxide nanoparticles (Axelbaum, 2000). In the SFE process, vapor-phase sodium reacts with a gaseous metal halide to produce an aerosol core material and salt (Figure 1). A variety of materials have been synthesized by the sodium/halide chemistry, including Ta, Ti, Al, Nb, Si, W, Fe, AlN, TiB$_2$, TiN, W–Ti alloys, and Al-AlN
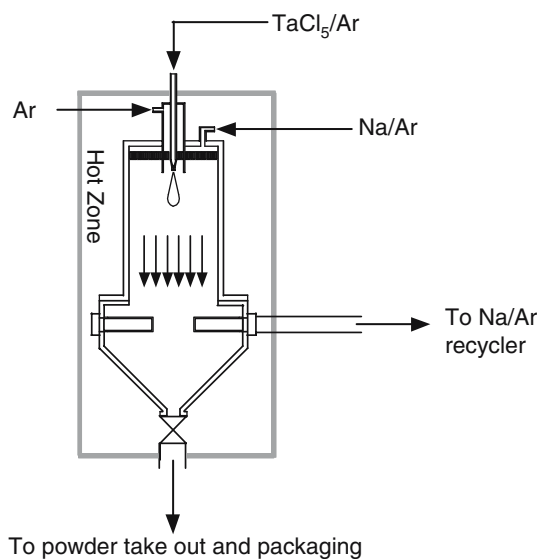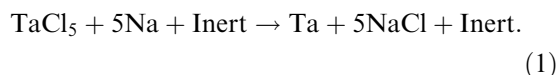

Figure 1. Schematic diagram of flame reactor for the sodium/halide flame and encapsulation process.

composites, and particle sizes from a few nanometers to hundreds of nanometers have been obtained (Axelbaum et al., 1995, 1996; DuFaux & Axelbaum, 1995). The following reaction is an example of the chemistry used in the synthesis of Ta:

$$TaCl_5 + 5Na + Inert \rightarrow Ta + 5NaCl + Inert.$$

(1)

The salt by-product makes it possible to obtain a level of control over core particle size and agglomeration, and prevent environmental contamination of core particles. Initially, core particles (e.g., Ta) are produced at the flame and grow by coagulation while the salt remains in the vapor phase. With heat loss the salt condenses onto the core particles, and as the salt-encapsulated particles grow, uncoated core particles are scavenged by the salt particles (Figure 2). Particle size can be controlled by modifying temperature and heat loss. The salt provides a relatively impermeable barrier, which controls the contact between core particles and environmental contaminants such as moisture and oxygen. The SFE process can also minimize intrinsic oxygen content by employing reactants that are free of oxygen. Figure 3 shows the morphology of a salt-encapsulated Ta nanopowder. The figure shows core particles of Ta (dark interior structure) within the salt encapsulate
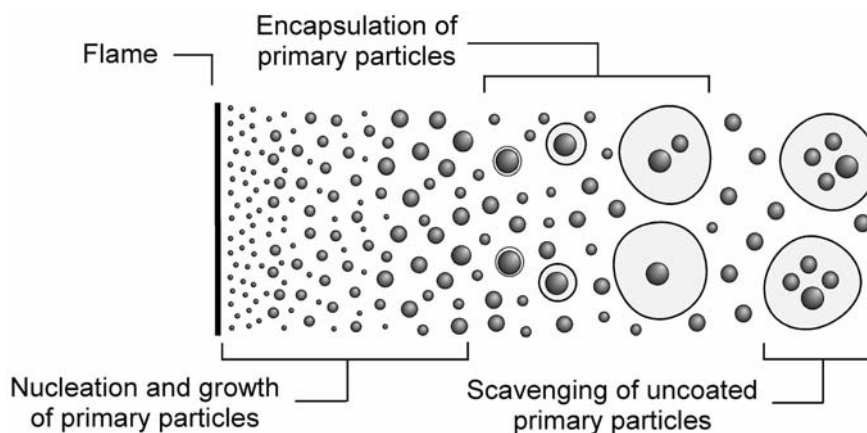
Figure 2. Illustration of particle dynamics associated with the sodium/halide flame and encapsulation process. Primary particles are produced in the flame zone and are subsequently encapsulated in salt.

Figure 3. TEM image of salt-encapsulated tantalum nanopowders produced using the SFE process. The Ta core particles are dark while the salt encapsulate is the light exterior structure.

(light exterior structure). To realize the full benefit of the pure nanostructured core material it is essential that the salt encapsulate, which protects the core particles during storage, be completely removed and the core particles rendered non-reactive (passivated or densified). The primary goals of this work are to demonstrate that the NaCl encapsulation material can be completely removed from the core particles in a manner that is consistent with established technology for powder processing and the microstructure of the exposed powder can then be altered, if desired. Both tasks can be accomplished without handling or exposure to air between the time the encapsulate is removed and the desired microstructure is obtained.

The material selected for this study is Ta. Tantalum is a refractory metal with many valuable properties (Moser, 1999), including excellent fabricability, a low ductile to brittle transition temperature ($-250°C$) and a high melting point ($2996°C$). Tantalum also has excellent corrosion resistance to many acids, most aqueous solutions of salts, organic chemicals, and various combinations of these agents.

The main use of Ta is in electronic capacitors (Gill, 1996; Kemet, 1996). The Ta capacitor market is a growing market fueled by telecommunications, cellular phones, automotive applications, and computers. For this application, Ta powder is the primary product used for anodes. The powder, which consists of agglomerates, is sintered to yield a porous structure with a high surface area. An amorphous pentoxide surface layer, which gives the Ta anode its capacitance, is formed electrolytically and has predictable growth. Additionally, the anodic film is stable at high temperatures (below approx. 2000°C). The specific capacitance increases with decreasing particle size due to the increase in specific surface area of the sintered material. Thus, the industry has been pushing to lower the primary particle size of the agglomerates that make up the capacitor anodes.
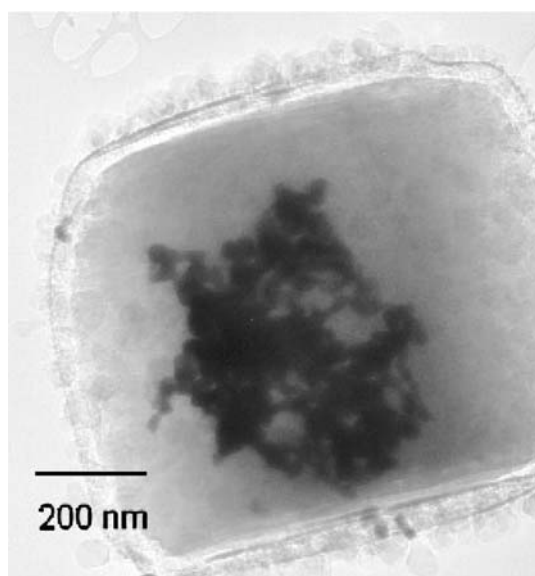
Ultrafine Ta powders can suffer from excessive oxygen contamination due to their large specific surface area. Furthermore, since the quality of the pentoxide layer depends on the purity of the underlying material, it is crucial that the starting powders have a high purity. High purity is also essential since impurities promote leakage. The SFE process allows the core Ta particles to retain their purity and small size, which makes the process uniquely suited for meeting the needs of the capacitor industry.

Encapsulate removal

One approach to removing NaCl is by vacuum sublimation. Sodium chloride has a reasonable vapor pressure at moderate temperatures (2.4 Torr at 746.9°C) (Kaufman, 1960). This allows NaCl to rapidly sublime at temperatures below those at which high melting point materials sinter, thereby avoiding grain growth and preserving the purity of the core particles. Thus vacuum sublimation is very attractive when the encapsulated powders are highly sensitive to contamination by air or water, especially for high melting point materials such as ceramics and refractory metals.

Although the potential for rapid NaCl sublimation exists, the temperature at which the salt is sublimed must be controlled so that the rate of vaporization is controlled. Excessive vaporization rates could result in entrainment of the extremely fine nanoparticles and subsequent ejection from the die. However, the time for sublimation must obviously be minimized and the salt completely removed, both of which are improved at higher temperatures. Thus, a sublimation temperature which allows reasonable vaporization rates without unnecessary entrainment of particles must be determined. Once the majority of the NaCl has been sublimed, an additional heat treatment at higher temperatures can promote more complete removal of residual encapsulate material.

Tantalum powders provide an excellent paradigm for demonstrating the feasibility of encapsulate removal and provide a solution to the difficult problem of producing non-oxide nanostructured consolidates. Production of Ta via the sodium/halide reaction overcomes problems of oxygen contamination through the use of oxygen free reactants and NaCl encapsulation. The high

sintering temperature of Ta allows vacuum sublimation of the salt encapsulate over a range of temperatures, while preserving the nanostructure and high specific surface area of the powder. Accommodating all of these demands presents an opportunity to utilize several of the benefits of encapsulated nanopowders: enhanced sintering rates, protection from contamination, and ultrafine grain size.

Experimental setup

Tooling for processing salt encapsulated nanopowders was designed so that sublimation would not be impeded and so that a sample of appropriate size could be created and removed easily. The tooling consists of an integrated press ram and tooling ram, and die. The ram is held in place slightly above the die during salt sublimation so that sublimation occurs with little restriction on sublimation rate. With this design, it is also possible to compact powder after sublimation. The salt encapsulated powders were packed to a tap density of roughly 55%.

The hot press is a standard vacuum hot press with a graphite furnace, manufactured by Elatec Technology Corporation, Haverhill, MA, capable of temperatures in excess of 2000°C. The press has a debindering system similar to that used to remove binders in conventional powder metallurgy processing. For the SFE powder, the encapsulate behaves as the binder. As shown schematically in Figure 4a, the debindering system allows the encapsulate component of the powder to be removed by vacuum sublimation while directing the encapsulate out of the hot press with an inert flow gas. This process reduces the possibility that the salt encapsulate will be a source of contamination since the salt condenses outside of the hot press, away from the hot zone, tooling, and powder. If desired, the powder can be hot pressed after the salt encapsulate (binder) has been removed (Figure 4b).

Experimental results

Sublimation studies

A typical X-ray diffraction (XRD) spectrum of as-produced salt-encapsulated Ta nanopowder is
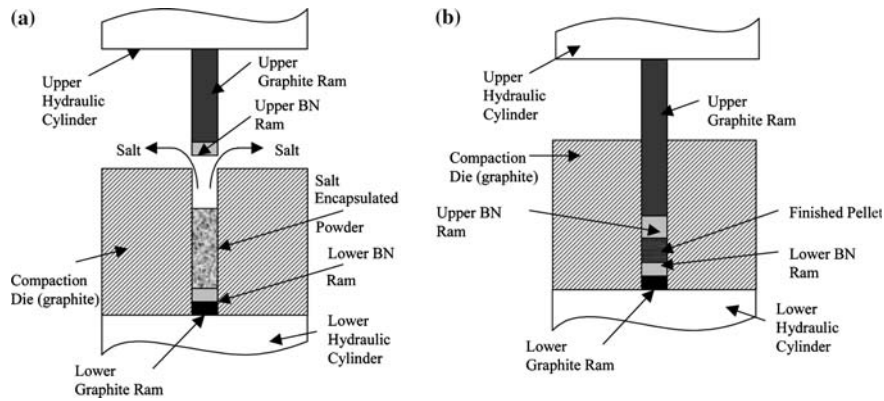
Figure 4. Schematic diagram of hot press with debinder capabilities showing sequential (a) salt removal and (b) consolidation.

shown in Figure 5. In addition to NaCl and body-centered cubic (BCC) Ta peaks, the XRD also shows a body-centered tetragonal (BCT) phase of Ta. Typical grain sizes for Ta in the salt encapsulated nanopowder are between 25 and 40 nm as determined by Scherrer formula examination of the XRD. The Scherrer formula relates crystallite size (L) to X-ray wavelength (λ), the Bragg angle (θ) and peak broadening (B). The method used in this study included correction factors for instrument broadening and broadening associated with lattice strain (Suryanarayana & Norton, 1998).

The die and ram are composed of graphite with boron nitride sleeves to avoid exposing the powder directly to graphite, which can lead to the creation of carbide phases at elevated temperatures. Sublimation experiments, performed with a 1.27 cm diameter die, show that the salt sublimation rate decreases with the addition of argon flow gas (refer

to Figure 4a). With argon flow through the chamber, the chamber pressure increases, which reduces the sublimation rate of the salt. The sublimation rate was experimentally determined as a function of temperature and with a fixed argon flow rate of 555 sccm. In the temperature range of 740–860°C the sublimation rate exponentially increased from 0.053 to 1.6 g/min. Considering the ramping rates and the mass of powder being processed, a reasonable control of salt removal rate is obtained at 785°C, using 555 sccm of argon. These conditions correspond to a chamber pressure of about 1 Torr and a sublimation rate of 0.132 g/min. This primary sublimation procedure is used in processing all samples unless noted otherwise. Greater than 99% of the salt mass can be removed from the salt-encapsulated Ta nanopowder in this manner. Examining the powder by Scanning Electron Microscopy (SEM) shows that a second phase is
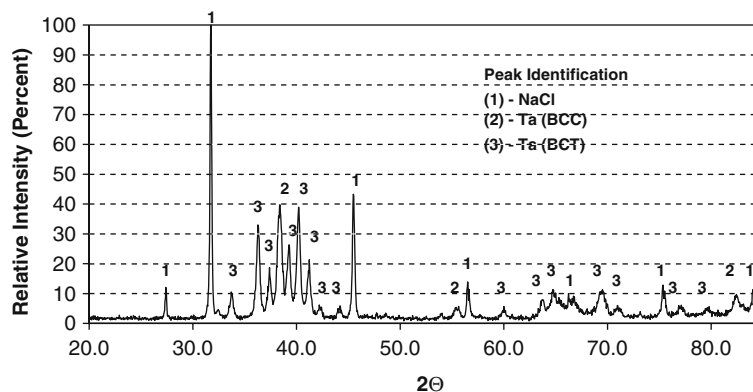

Figure 5. XRD spectrum of Ta/NaCl powder showing NaCl, BCC-Ta and BCT-Ta.

present after primary encapsulate removal, and Energy Dispersive Spectroscopy (EDS) indicates that this second phase consists primarily of Na and Cl, which is indicative of residual encapsulate. In order to expedite the complete removal of the salt, elevated-temperature soaks ($>785°C$) were performed under high vacuum ($\sim10^{-5}$ Torr) without flow-gas. Table 1 shows experimental run conditions and elemental analysis for the samples discussed. The temperatures for the primary sublimation (column 2) were measured in the powder with a type K thermocouple while those labeled residual sublimation/sintering (column 4) were measured in the workbox with a type C thermocouple. Due to temperature limitations of the type K thermocouple, direct measurements of the powder were not possible for the sintering studies. A workbox temperature of 880°C corresponds to a powder temperature of 785°C. The difference between the workbox temperature and the powder temperature decreases with increasing temperature.

For 30 min hold times and a workbox temperature of 930°C ($\sim830°C$ powder temperature) or below (samples A, B, C), a secondary phase is present in the powder, as shown in Figure 6. By increasing the workbox temperature to 1000°C and holding for 120 min (sample D) there is no indication from SEM of an encapsulate phase (Figure 7). EDS of the sample, shown in Figure 8, also indicates the presence of only Ta. The Cl level in sample D as measured by Glow Discharge Mass Spectrometry (GDMS), is 21 ppm, confirming

complete NaCl removal. The Na concentration is 444 ppm, with total metallic impurities at 2908 ppm as determined by Inductively Coupled Plasma – Atomic Emission Spectroscopy (ICP-AES) (Table 1). A typical X-ray diffraction pattern of the resulting Ta nanopowder obtained in this manner is shown in Figure 9. A Comparison with Figure 5 shows that the NaCl and BCT Ta phases have been removed and only the BCC Ta phase remains. Also of note is the absence of any oxide phase in the sample.

When residual hold temperatures are 1200°C or greater for 120 min (samples E, F, and G) both Na and Cl concentrations are reduced below 5 and 20 ppm, respectively, which were the detectable limits of ICP-AES and GDMS. The total metallic impurities are also reduced with increasing temperature. A residual hold of 1200°C for 120 mins (sample E) reduced the total metallic impurities to 424 ppm as determined by ICP-AES. At 1400 and 1600°C residual holds (sample F and G) the total metallic impurities are 434 and 224 ppm, respectively, indicating some purification at higher temperature.

Sintering studies

Pressureless sintering is the simplest consolidation process because it allows for densification solely by thermal means. This process is typically used for materials that densify easily. Adding heat to

Table 1. Processing conditions for samples salt-encapsulated tantalum and elemental analysis for processed samples

Sample ID	Primary sublimation 1 Torr, 555 sccm argon		Residual sublimation/ sintering 10^{-5} Torr		Cl via GDMS (ppm)	Na via ICP-AES (ppm)	Total Metals via ICP-AES (ppm)
	Temperature *(°C)	Time (min)	Temperature *(°C)	Time (min)			
A	785	150	N/A	N/A	Not tested	Not tested	Not tested
B	785	150	880	30	Not tested	Not tested	Not tested
C	785	150	930	30	Not tested	Not tested	Not tested
D	785	150	1000	120	21	444	2908
E	785	150	1200	120	$\leqslant20$	$\leqslant5$	424
F	785	150	1400	120	$\leqslant20$	$\leqslant5$	434
G	785	150	1600	120	$\leqslant20$	$\leqslant5$	224
H	785	150	1600	210	Not tested	Not tested	Not tested

*Temperature for primary sublimation was measured on the bottom ram, near the powder and indicates a true powder temperature. Due to experimental limitations, the higher temperatures associated with residual sublimation were measured with a type C thermocouple *in the workbox*. Due to heat loss, the workbox temperature is typically higher than powder temperature by 100°C or less.
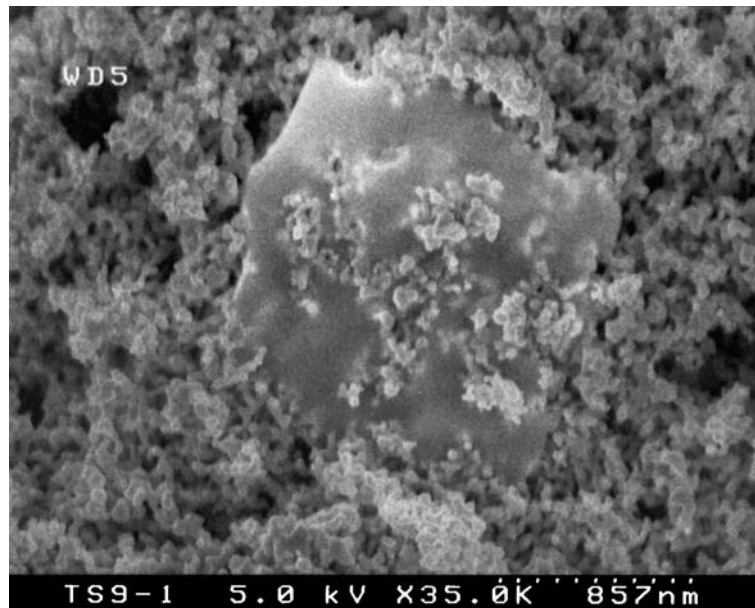
Figure 6. SEM micrograph detailing ultrafine Ta powder and large residual salt structure (sample C) processed with heat treatment at 930°C (∼830°C powder temperature) for 30 min under high vacuum.
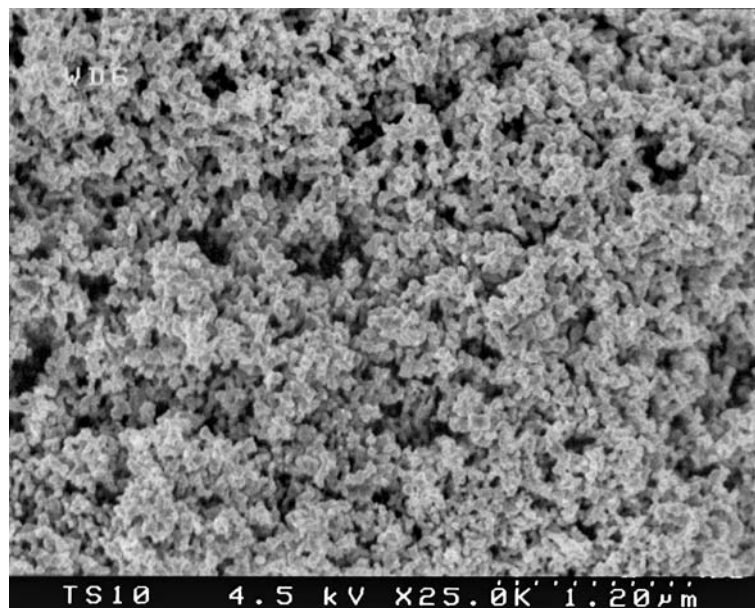

Figure 7. SEM of encapsulate-free ultrafine Ta powder (sample D) processed with heat treatment at 1000°C for 30 min under high vacuum.

increase the powder temperature overcomes the activation energy of the particles, causing a reduction of surface free energy by coarsening of the microstructure and densification. At the same time coarsening reduces the driving force for densification due to the corresponding reduction
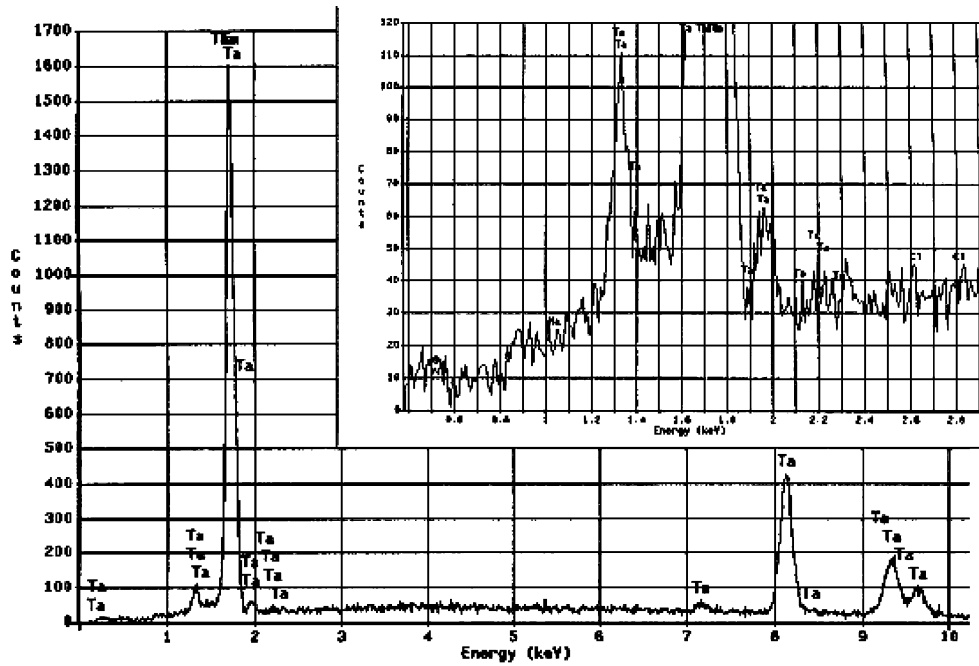
Figure 8. EDS of encapsulate-free Ta surface (sample D). Inset details absence of NA and Cl from the spectrum.

of surface free energy (Morris & Morris, 1997). For micron-sized powders, temperatures that are 75% of the melting temperature of the material are typically needed to create a dense consolidate. This corresponds to a sintering temperature of approximately 2250°C for micron-sized Ta. Key factors affecting sintering rate are temperature and particle size. Increased sintering rates are achieved with smaller particles and higher temperatures.

Samples heat-treated at or below 1000°C for 120 min or less (samples A, B, C and D) show little

evidence of particle coarsening. For sample D, particle sizes measured from SEM are between 60 and 100 nm and the specific surface area is 12.2 m^2/g, as determined by BET. These powders appear to be below the temperature required to activate a significant amount of atomic diffusion. As shown in Figure 10 for sample E, when the exposed core particles are heat-treated at 1200°C for 120 min the particle sizes increase to as large as 250 nm and the specific surface area is reduced to 6.9 m^2/g. At 1400°C the particle size increases to
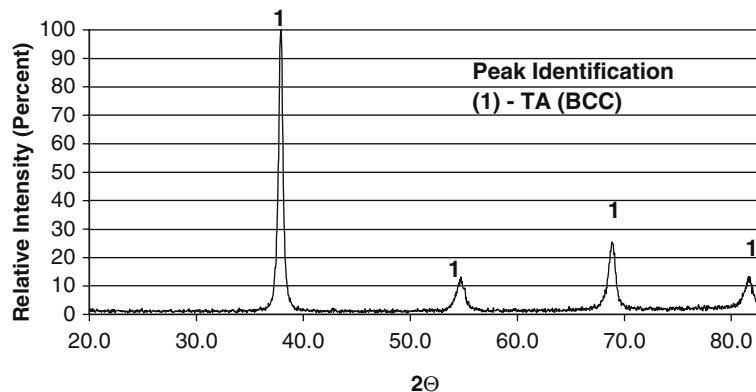

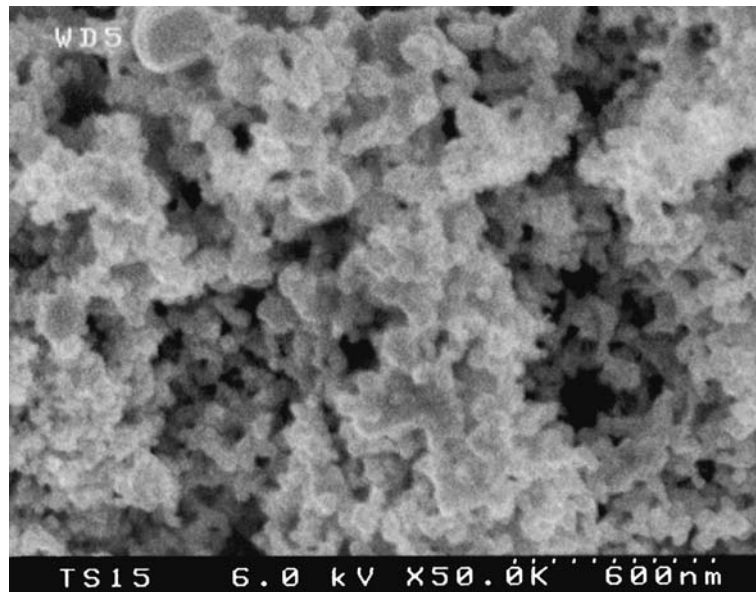*Figure 9.* XRD of Ta produced using the SFE process and with the encapsulate removed via vacuum sublimation.

Figure 10. SEM micrograph of sample E, residual heat-treated at 1200°C for 120 min.
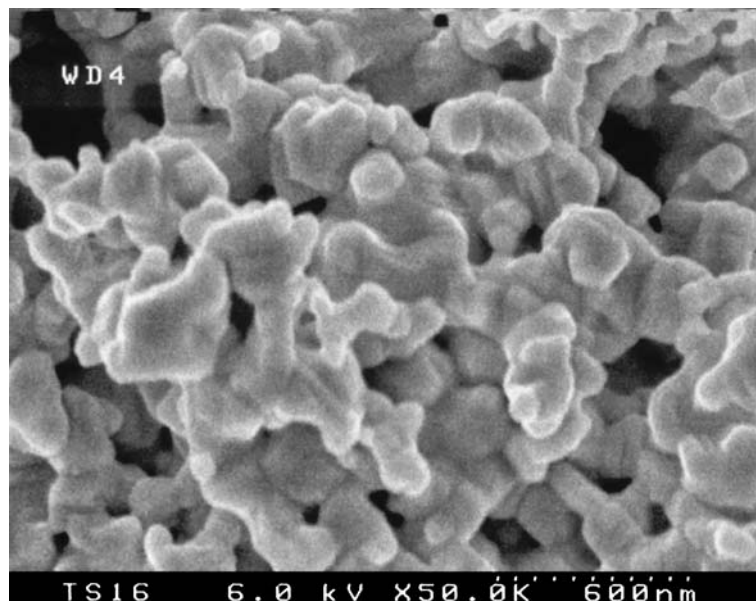

Figure 11. SEM micrograph of sample F, heat-treated at 1400°C for 120 min.

as large as 400 nm for a 120 min hold (sample F, Figure 11). Heat treating the core particles at 1600°C for 120 min not only coarsens the particles, but also sinters them into a cohesive body with grain sizes larger than 3 µm (sample G, Figure 12).

Sample H was hot pressed in a 2.54 cm diameter die with 45 MPa pressure, applied uniaxially for
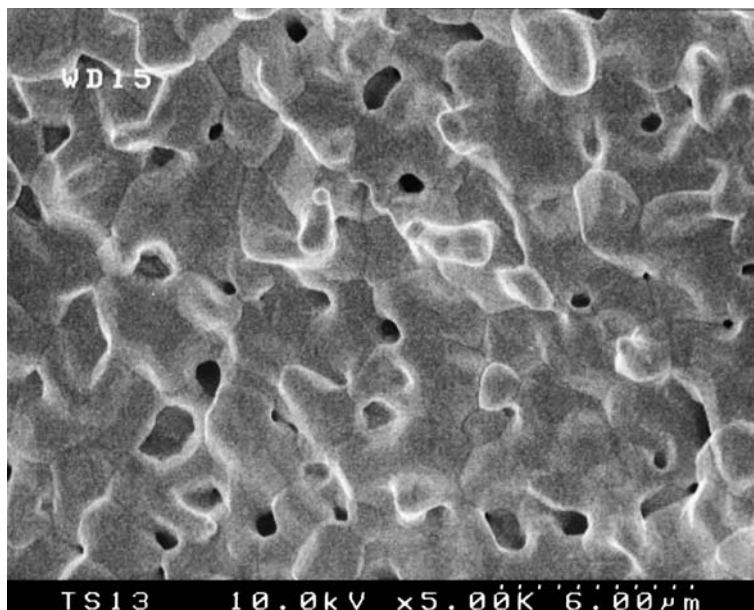
Figure 12. SEM micrograph of sample G, heat-treated at 1600°C for 120 min.

210 min during the 1600°C heat treatment. As outlined in the experimental setup, Figure 4 show a schematic of the process that allows for sublimation followed by hot pressing. The sample was found to be 98% theoretically dense as measured by Archimedes principle in toluene using the formula

$$\rho_S = \rho_T * \left(\frac{m_a}{m_a - m_t} \right) \qquad (2)$$

where ρ_S is the sample density, ρ_T is the density of toluene, m_a is the mass of the sample measured in air and m_t is the apparent mass of the sample measured in toluene. SEM images of the unetched surface show no signs of porosity. A portion of the sample was polished and etched with a solution of 1 part 50% HF, 1 part HNO_3, 2 parts glycerol (Figure 13) to expose the microstructure (Hirsch et al., 1965). As observed in the SEM shown in Figure 13, large grains (2–4 μm), comparable to those observed for the sintered material (sample G) are obtained.

Summary and conclusions

Processes for removing the encapsulate from salt-encapsulated Ta particles (created by the SFE process) using a standard hot press and debindering system were examined. It was found that with a two step process where first the bulk of the salt is sublimed from the core particles at 785°C and directed out of the system with an inert gas flow, and next the resulting powder is exposed to a high-vacuum for 120 min at a workbox temperature of 1000°C, the salt could be removed to 21 ppm Cl. The salt is collected outside of the system, with no evidence that it affects the core particles. By processing salt-encapsulated nanopowders in this manner it was possible to remove the encapsulate while retaining the nanostructure and purity of the core particles. The EDS, XRD, GDMS, and ICP-AES results indicate removal of Na and Cl to below detectable limits for samples held at a workbox temperature of 1200°C or more for 120 min. After complete salt encapsulate removal, processed powders with specific surface area as high as 6.9 m²/g (sample E) can be achieved. By heat treating the core particles between 1200 and 1600°C and holding for 120 min the sintering behavior of the powder has been studied. By avoiding exposure to oxygen, these results indicate fundamental sintering behavior of nano Ta. The total metallic impurities for sintered Ta created from processed salt-encapsulated nanopowder with a 120 min residual hold at
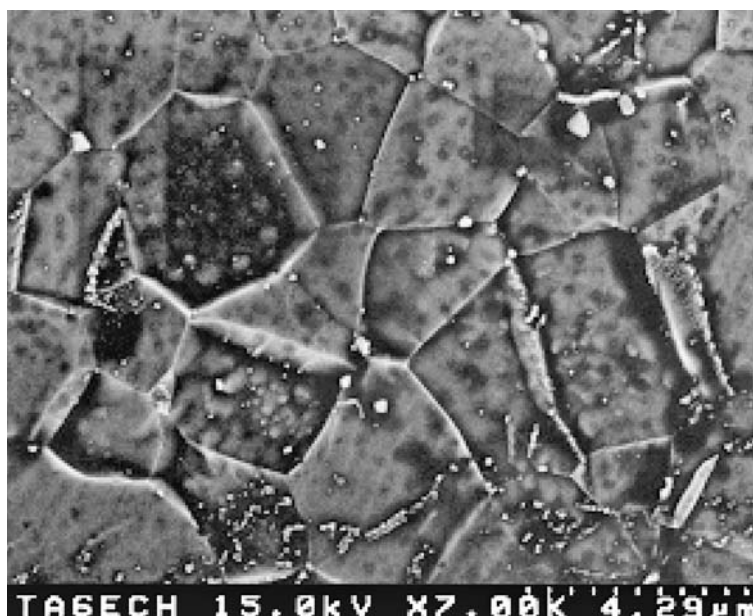
Figure 13. SEM micrograph of sample H, heat-treatment at 1600°C for 210 min. Full density is accomplished with an applied pressure of 6.5 ksi.

1600°C is 260 ppm as determined via ICP-AES. Nano-tantalum achieved full density at 1600°C under a uniaxial load of 45 MPa pressure with a 210-min hold time.

References

Andrievski R.A., 1994. Compaction and sintering of ultrafine powders, Int. J. Powder Metall. 30(1), 59–66.

Axelbaum R.L., 2000. Synthesis of stable metal and non-oxide ceramic nanoparticles in sodium/halide flames, Powder Metall. 43(4), 323–325.

Axelbaum, R.L., DuFaux, D.P. & Rosen, L.J., 1995. Method and Apparatus for Producing High Purity and Unagglomerated Submicron Particles. U.S. Patent No. 5498446.

Axelbaum R.L., C.R. Lottes, J.I. Huertas & L.J. Rosen, 1996. Gas-phase combustion synthesis of aluminum nitride powders, Proc. Combust. Inst. 26, 1891–1897.

Cho H., M.A. Waters & R. Hogg, 1996. Investigation of the grind limit in stirred-media milling, Int. J. Mineral Proc. 44–45, 607–615.

Cox, D.M., 1999. WTEC Panel Report on Nanostructure Science and Technology: R & D Status and Trends in Nanoparticles, Nanostructured Materials, and Nanodevices: Final Report: December 1998. 49–66.

DuFaux D.P. & R.L. Axelbaum, 1995. Nanoscale unagglomerated nonoxide particles from a sodium coflow flame, Combust. Flame 100(3) 350–358.

Gill J., 1996. Basic Tantalum Capacitor Technology. AVX Technical Information Articles. England: AVX Corporation.

Groat E.A. & T.J. Mrox, 1994. Aqueous slip casting of stabilized AIN powders, Am. Ceramic Soc. Bull. 73(11), 75–78.

Groza J.R. & R.J. Dowding, 1996. Nanoparticulate materials densification, Nanostruct. Mater. 7(7), 749–768.

Haber J.A. & W.E. Buhro, 1998. Kinetic instability of nanocrystalline aluminum prepared by chemical synthesis; Facile room-temperature grain growth, J. Am. Chem. Soc. 120(42), 10847–10855.

Hirsch P.B., A. Howie, R.B. Nicholson, D.W. Pashley & M.J. Whelan, 1965. Electron Microscopy of Thin Crystals. London: Butterworths.

Jena P., S.N. Khanna & B.K. Rao, 1996. Stability and electronic structure of cluster assembled materials, Mater. Sci. Forum 232, 1–25.

22

Kaufmann D.W., 1960. Sodium Chloride, The Production and Properties of Salt and Brine. New York: Reinhold Publishing Corp.

Morris D.G. & M.A. Morris, 1997. Hardness, strength, ductility and toughness of nanocrystalline materials, Mater. Sci. Forum 235–238, 861–872.

Moser K.D., 1999. The manufacture and fabrication of tantalum, J. Minerals Metals Mater. Soc. 51(4), 29–31.

Shriver D.F. & M.A. Drezdzon 1986. The Manipulation of Air-Sensitive Compounds, JohnWiley & SonsNew York.

Suryanarayana, C. & Norton, M.G., 1998. X-Ray Difrraction: A Practical Approach. Plenum Publishing Corporation, pp. 207–221.

Weissmuller, J., 1996. Nanocrystalline Materials, an Overview. The Minerals Metals, and Materials Society, pp. 3–19.

Zhang H., R.L. Penn, R.J. Hamers & J.F. Banfield, 1999. Enhanced adsorption of molecules on surfaces of nanocrystalline particles, J. Phys. Chem. B 103(22), 4656–4662.